



# Three-dimensional Electrocoagulation Process Optimization Employing Response Surface Methodology that Operated at Batch Recirculation Mode for Treatment Refinery Wastewaters

Samar K. Theydan <sup>a,\*</sup>, Wadood T. Mohammed <sup>a</sup>, SK Manirul Haque <sup>b</sup>

<sup>a</sup> Department of Chemical Engineering, Collage of Engineering, University of Baghdad, Baghdad, Iraq

<sup>b</sup> Department of Chemical Engineering, Jubail Industrial Collage, Al-Jubail, Saudi Arabia

## Abstract

The performance of a three-dimensional electrocoagulation process operated at a batch recirculation mode for treating petroleum refinery wastewater using aluminium as a sacrificial anode, stainless steel as a cathode, and granular activated carbon with metal impregnated carbon (GACMI (Al: Fe)) with mass ratio (2:1) as a third particle electrode was investigated. Effects of operating factors such as the applied voltage (15-30 v), flow rate (50-175 mL/min), pH (4-10), and GACMI dosage (5-10) g/L on the chemical oxygen demand removal were investigated. Using Box-Behnken design (BBD), a mathematical model relating the essential operational parameters to chemical oxygen demand (COD) reduction was constructed. Results showed that the effect of GACMI dosage on the efficiency of COD removal was the major one, where COD removal increased as GACMI dosage increased. However, increasing applied voltage would enhance the performance of the electrocoagulation reaction. Experimental chemical oxygen demand removal of 96.25 % was attained at the optimized conditions (applied voltage=27.7 v, flow rate=128 mL/min, pH=5.6, GACMI dosage= 8.7 g/L). BET-specific surface area, total pore volume, X-ray fluorescence (XRF), energy-dispersive X-ray spectroscopy (EDX), and scanning electron microscopy (SEM) were employed for the characterization of GACMI particle electrodes.

*Keywords:* three-dimensional electrocoagulation; response surface methodology; batch recirculation mode; refinery wastewaters.

*Received on 18/01/2023, Received in Revised Form on 03/06/2023, Accepted on 03/06/2023, Published on 30/03/2024*

<https://doi.org/10.31699/IJCPE.2024.1.6>

## 1- Introduction

Over the next two decades, there will be a 44% increase in the world's energy demand [1], making the production of petroleum effluent and the processing of petroleum, which is a complex mixture of organic liquids known as crude oil and natural gas, an essential concern [2]. The refineries were divided into two categories: hydro-skimming units, which include crude distillation units, desulphurizing units, and reforming units, and complex units, which also contain catalytic cracking units [3]. According to the current decade's average global oil output, around 300 L of wastewater must be produced for every oil barrel, meaning the global oil sector produces approximately 34 million barrels of polluted water daily [4, 5]. Furthermore, the oil industry will likely continue producing and discharging tainted sewage, given the rapid rise in global oil consumption. Oil effluent has a variety of chemical compositions depending on its source. Because of global warming, the effects of oil wastewater are getting worse as freshwater resources on Earth rapidly disappear [6, 7]. The amount of dissolved oxygen bacteria need to survive, 2 mg L<sup>-1</sup> of dissolved oxygen, is reduced when petroleum wastewater with a high organic content is discharged into an aquatic environment. Unpleasant

colors and scents are produced in water in anaerobic systems by the byproducts of chemical and biological reactions. In order to lessen that, it is crucial for water to have oxygen [8].

Additionally, these pollutants contaminate the soils of gas stations and refineries, the bed soils of rivers and lakes, and other areas. This necessitates pricey remedial procedures. These contaminants affect human health by causing significant illnesses or poisoning consequences [9]. The need for effective treatment technologies is growing more due to the ongoing growth in climate change, which increases freshwater demand and the amount of contaminated runoff in other parts of the world [10].

Conventional wastewater treatment techniques, such as gravity separation and skimming, air flotation, coagulation, de-emulsification, and flocculation, have inherent drawbacks like low efficiency, high operating costs, and corrosion and produce significant amounts of secondary pollutants (such as chloride and sulfate in the coagulation-precipitation process) and large volumes of sludge or waste that pose serious environmental issues [11, 12]. Due to their high salt concentration, it is impracticable to evaporate these solutions in ponds [13].



\*Corresponding Author: Email: [samar.kareem@coeng.uobaghdad.edu.iq](mailto:samar.kareem@coeng.uobaghdad.edu.iq)

© 2024 The Author(s). Published by College of Engineering, University of Baghdad.

This is an Open Access article licensed under a [Creative Commons Attribution 4.0 International License](https://creativecommons.org/licenses/by/4.0/). This permits users to copy, redistribute, remix, transmit and adapt the work provided the original work and source is appropriately cited.

Due to the partial blockage of biodegradation, even biological processes are ineffective in curing PRW. It might be brought on by sulfide, interfering with the biosystems' ability to transmit oxygen [14]. Also, standard treatment methods cannot completely remove emulsified oil or tiny oil droplets [15]. However, these processes have drawbacks that electrochemical techniques can overcome. To remove hydrocarbons and other organic matter from petroleum refinery wastewater, different manners were used, such as chemical coagulation-precipitation [16], electrochemical processes, such as electrooxidation and electrocoagulation [17-19], biological treatment [20, 21], activated sludge adsorption [22], a combination of solvent extraction and freeze-thaw [23], photo-degradation [24], and the Fenton and photo-Fenton processes [15].

The three main treatment procedures in electrochemical processing are electrooxidation, electrocoagulation, and electro-flotation. Successful methods for extracting oils from wastewater include electrocoagulation and electro-flotation in particular. The kind of electrode utilized during treatment denotes the process type for electrochemical treatment. Electrocoagulation occurs when a soluble metal such as iron or aluminium is employed as the anode; oxidation and floatation occur when an insoluble inert electrode is used as the cathode [25]. The primary reactions that occurred throughout the electrolysis process were the ion transfer of dissolved metal into the water through oxidation in the anode and the generation of H<sub>2</sub> gas and hydrolysis of water through reduction in the cathode [26]. Monomeric and polymeric metal hydroxide flocs are created depending on the solution pH after these procedures. Through adsorption, precipitation, and floatation, these metal hydroxide flocs enable the separation of contaminants from the ambient environment and are highly effective at eliminating pollutants from wastewater [27]. The most notable benefits of the process include minimal equipment requirements, simple operation, quick process times, no chemical use, and low sludge production [28, 29]. The treatment of wastewater containing finely distributed particles using electrocoagulation has received much attention recently. This technology can potentially replace sophisticated methods that need significant quantities of chemicals due to its strength and mobility [30].

Single electrodes like Iron-Iron and Aluminium-Aluminium, or coupled electrodes like Aluminium-Iron or Iron-Aluminium, which are referred to as a two-dimensional electrode system, have been widely used in the traditional electrocoagulation approach to treat water and wastewater [31]. According to reports, mixed Aluminium-Iron or Iron-Aluminium electrodes operate better than single electrode systems, eliminating contaminants with higher efficiency [32]. However, there are certain restrictions on how these two-dimensional electrodes may be employed, including the short lifespan of the electrode and the low current efficiency caused by the electrode's low conductivity [33, 34]. Utilizing three-dimensional (3D) electrodes with activated carbon or

metal particles can alleviate these drawbacks in two-dimensional electrode (2D) techniques [35].

As an alternative, a three-dimensional electrode approach utilizing carbon particles has gained traction recently. It has been demonstrated to be effective in removing chloramphenicol and increasing the specific surface area of the working electrode [36], ions of metal removal [37], and removal of cyanide [38], as well as the most recent removal of organic contaminants like phenols [39], dyes [40, 41], tetracycline [42] and Furfural [43]. Three-dimensional electrocoagulation is thus predicted to be an excellent solution for petroleum refinery wastewater treatment. Box-Behnken design (BBD) is a set of statistical methods approximating a functional connection between a response and a set of influencing variables. It may also be used to optimize multifactor operations by examining the combined influence of various variables on the response. The Box-Behnken experimental design is often used to optimize many treatment operations [44, 45].

This study investigates the efficacy of a three-dimensional electrocoagulation process to remediate refinery effluent utilizing a recirculating batch mode. The impacts of applied voltage, flow rate, pH, and GACMI dosage on (COD) removal efficiency were explored using the Box-Behnken design(BBD) by building a mathematical model and producing three-dimensional response surface graphs. Finally, the response model was used to optimize affecting factors. The elimination of chemical oxygen demand (COD), and turbidity from refinery wastewater at the optimal parameters predicted by the Box-Behnken design was confirmed using experimental findings.

## 2- Materials and Methods

### 2.1. Materials and Experimental Work

Al-Dura Refinery, a petroleum refinery in southern Baghdad, Iraq, donated an 80-liter sample of its processed wastewater. The refinery effluent sample was utilized untreated. It was collected from the feeding tank before the biological treatment facility and kept in closed containers at 4°C until usage. The characteristics of this sample are presented in Table 1. The insufficient conductivity of raw water causes the cell potential to rise. Thus, to increase the conductivity, supporting electrolytes must be added. The conducting of 12.16 mScm<sup>-1</sup>, within the range required to achieve low cell potential [46], was obtained using Na<sub>2</sub>SO<sub>4</sub> at 0.025 M and NaCl at 0.0625 M as supporting electrolytes.

Hydrochloric acid (HCl, 37%, liquid, Sigma-Aldrich) and Sodium hydroxide (NaOH, ≥ 97%, pellets, Sigma-Aldrich) were used to prepare a 1M solution for adjusting the initial pH of the treated wastewater.

A commercial granular activated carbon was used, and its physical properties are shown in Table 2. Ferric chloride anhydrous (FeCl<sub>3</sub> powder with 98% purity by weight, Alpha Chemike company, and Aluminium chloride anhydrous (AlCl<sub>3</sub> powder with 98 % purity by

weight, Central Drug House Ltd. Comp.) were used as metal sources for the metal impregnation process.

**Table 1.** Characteristics of Al-Dura Oil Refining Wastewater Sample

Property	Value
pH (-)	6.8
COD (ppm)	1400
Conductivity (mS/cm)	4.03
Turbidity (NTU)	227
TDS(g/L)	2.07
F (ppm)	0.19
Cl <sup>-</sup> (ppm)	422.4
Zn-(ppm)	0.08
Cu (ppm)	0.025
Mn(ppm)	0.33
Ni(ppm)	0.5
Pb(ppm)	1
Cd(ppm)	0.1
Cr(ppm)	1

**Table 2.** Physical Properties of Commercial Granular Activated Carbon

Parameters	values
Test standard	ASTM-D
BET Surface Area m <sup>2</sup> /g	950-1200
Iodine Number mg/g	900-1150
Total ash content	Max. 5%
Hardness	Min. 97%
Apparent density Kg/m <sup>3</sup>	460±40
Moisture content	8% (as packed)
Attrition	Max. 3%
Particle size	8*30 mesh available

## 2.2. Granular Activated Carbon with a Metal-Impregnated (GACMI) Preparation

As explained by Theydan and Mohammed [47], Commercial GAC particles were washed with deionized distilled water to eliminate contaminant compounds after sieving them to a particle size of more than 1 mm in diameter. Finally, the particles were dried in an oven at 105 °C for 24 hours. Subsequently, the granular activated carbon was impregnated with mass ratio (2:1:10 as Al:Fe:AC) using AlCl<sub>3</sub> and FeCl<sub>3</sub> as a source for Al and Fe, respectively, then mixing with 50 ml deionized water at 90°C for 4 h. The final mixture was blended in a 500 ml round-bottom flask with two necks: one with a thermometer to gauge temperature and the other with a water-cooling reflux condenser, where the reaction occurred at ambient pressure. The flask was heated and agitated using an oil bath (engine oil with a flash point of 220 °C from Al-Dora refinery), where a homogenous solution was obtained by using a magnetic stirrer hot plate and rotating the mixture at a rate of 200 rpm. Once again, the granular activated carbon with a metal-impregnated (GACMI) was washed with deionized distilled water and dried for 24 hours at 105°C.

## 2.3. Experimental Procedure

The laboratory configuration depicted in Fig. 1 was used to carry out the tests [18]. A Perspex glass tube electrochemical reactor (Fig. 1 a and b) measuring 30 mm in diameter and 140 mm in height. Throughout the

duration of the experiment, a peristaltic pump (RUNZE, single-stage pump, built in China) was used to pump the wastewater to the cylindrical electrocoagulation cell. This improved the impact of the mixing parameter by ensuring that the solution was continuously recirculated between the electrodes. The stainless steel and aluminum disc electrodes have been connected to a DC power supply. A total of 7.065 cm<sup>2</sup> was the effective surface area of each electrode. Using raw granular activated carbon or GACMI as particle electrodes resulted in a fast electron transfer rate between the anode and the cathode, allowing the spacing between the electrodes to be 5 cm [48]. The wastewater was circulated from the aluminum anode to the cathode, where the anode was positioned below the cathode. A packed bed of GAC or GACMI was arranged between the anode and the cathode in the case of the 3D reactor. Throughout every experiment, a digital direct current power supply (UNI-T, UTP3315PF, with a voltage range of 0–30 volts and 0–5 amperes) was utilized to provide an appropriate voltage. A multimeter (A-meter and volt-meter) was used to measure the system's current and voltage. Each experiment used a multimeter to record each electrode's applied current and corresponding voltages. The electrocoagulation cell's overflow was fed back to the electrocoagulation unit after the effluent from the unit was transported to a cylindrical acrylic reservoir (200 mm in height, 100 mm in outside diameter, and 4 mm in thickness) with a matching cover (outside diameter of 120 mm and thickness of 10 mm). The reservoir has two access points: one at ground level, and another on the side, elevated some (50 mm) from the base, which is used for feeding the solution to the electrocoagulation cell. Every receptacle has its own PVC valve. Each outlet was provided with a PVC valve. The cover was provided with an inlet to recycle the solution from the electrocoagulation cell.

The electrodes were cleaned in acetone and 5% (v/v) HCl solutions (35%) to remove the oxide and passivation layers [49]. HCl solution (1M) and NaOH solution (1M) adjusted pH. NaCl and Na<sub>2</sub>SO<sub>4</sub> were used as an electrolyte. NaCl solution was utilized as an extra electrolyte because of its various benefits, which include the chloride ions' ability to significantly reduce the negative effects of other anions like HCO<sup>3-</sup> and SO<sub>4</sub><sup>2-</sup>. An insulating layer would be formed on the cathode surface by the precipitation of Ca<sup>2+</sup> or Mg<sup>2+</sup> ions brought on by the carbonate ion. The electrochemical cell's ohmic resistance would be significantly increased. At the same time, this insulating layer would substantially reduce its current efficiency and treatment conversion. Therefore, it is suggested that 20% Cl<sup>-</sup> be present among the current anions to permit proper EC activity in water treatment [50]. The ambient temperature for all tests was 25 ± 2 °C. Samples were filtered using 150 mm filter paper after the experiment before being analyzed. Total dissolved solids (TDS), pH, turbidity, and the initial and final chemical oxygen demand concentrations were also measured.

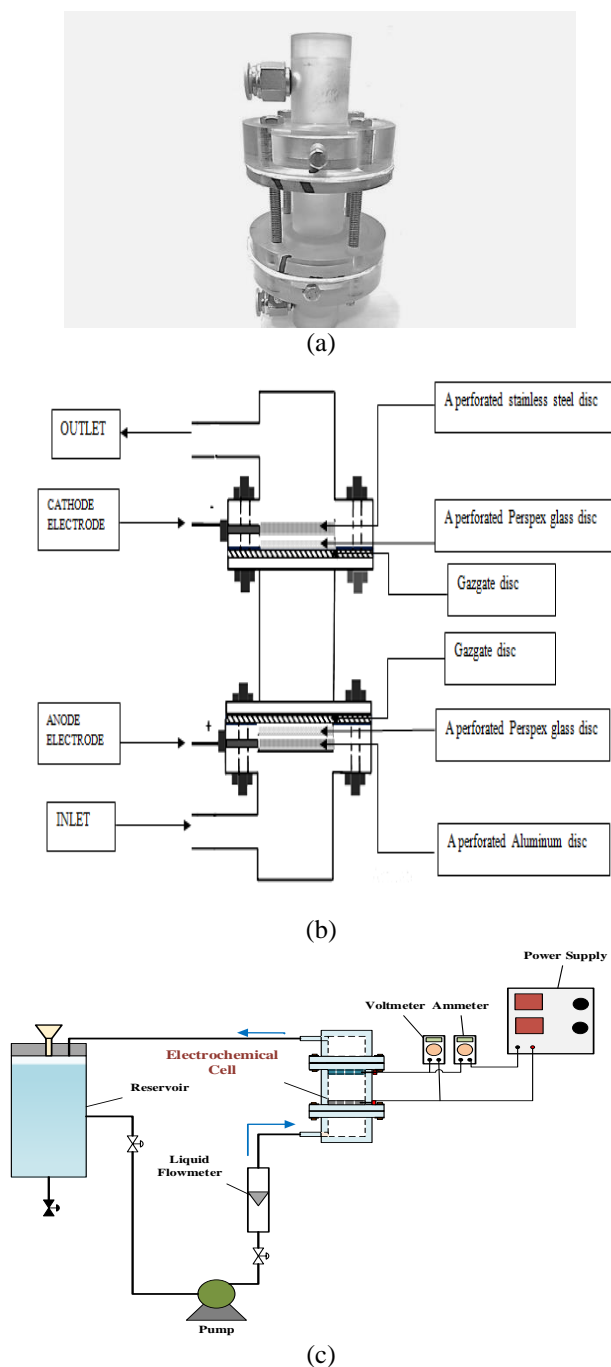


**Fig. 1.** (a) Photograph of the Electrocoagulation Cell (b) Schematic Diagram of Electrocoagulation Cell (c) Schematic Diagram of Electrocoagulation System

#### 2.4. Methods of Analysis

The Spectro Xepos X-ray fluorescence (XRF, Ametek Co., Germany) was utilized to investigate the textural features of both raw GAC and GACMI. Scanning electron microscopy (SEM) was also used to examine the morphology and microstructure. At the exact surface locations of the SEM, energy dispersive X-ray spectroscopy (INSPECT, F50, REI Co., Netherlands) was also used for surface element analysis. With the SA-9600 model (Horibe USA brand), physical characteristics (i.e.,

BET-specific surface area and total pore volume) were calculated using nitrogen gas as the adsorbate.

The Lovibond COD VARIO photometer was used for COD analysis with photometric detection (COD Setup, MD 200, UK). A 2 mL substrate sample was thermally oxidized in a cuvette tube using a standard oxidation reagent to measure the chemical oxygen demand (COD). A thermo-reactor (RD 125, Lovibond, Germany) was utilized to achieve thorough substrate oxidation, and chemical oxygen demand (COD) in mg/L was determined. The compact Lovibond® infrared turbidity meter Turbi Check was used for turbidity measuring. The turbidity and COD removal efficiency was evaluated based on Eq. 1, where  $C_i$  is the initial concentration ( $\text{mg L}^{-1}$ ) and  $C_f$  is the final concentration ( $\text{mg L}^{-1}$ ) [51]:

$$RE\% = \frac{C_i - C_f}{C_i} \times 100 \quad (1)$$

Energy consumption (EC) refers to the amount of electrical energy consumed throughout the EC process to remove one kilogram of COD. EC may be determined in terms of kWh/kg by using Eq. 2 [52]:

$$EC = \frac{U.I.t \times 1000}{(COD_i - COD_f)V} \quad (2)$$

The initial and final chemical oxygen demands (in mg/L) are denoted by  $COD_i$  and  $COD_f$ , respectively. The applied cell voltage (Volt), current (A), electrolysis duration (h), and effluent volume (L) are represented by  $V$ . The pH was measured using a (HANNA Instruments Co.) pH-meter. The total dissolved solids (TDS) was tested with a (161002 PurePro Inc.) TDS-meter. The (HANNA HI-99301) was used to measure electrical conductivity.

#### 2.5. Design of Experiments

The experimental design plays a crucial part in the development of the process. It may solve process problems to enhance performance [53, 54]. Response surface methodology (RSM) combines mathematical and statistical tools to develop models and analyze responses impacted by several variables, intending to optimize this response [55]. In this investigation, a 3-level, 4-factor Box–Behnken experimental design was utilized to verify and examine the parameters that controlled the elimination of COD. Applied voltage ( $X_1$ ), flow rate ( $X_2$ ), pH ( $X_3$ ), and GACMI dosage ( $X_4$ ) were considered process factors, while the response was RE% of COD. The coded scales of process factors were -1 (low level), 0 (middle or central point), and 1 (high level) [56]. The process parameters and their respective levels are presented in Table 3 and Table 4. For the 3-level factorial design, Box–Behnken builds and improves the designs necessary to obtain a viable quadratic model with the relevant statistical features while using just part of the required runs. The following equation can be used to compute the number of runs ( $N$ ) needed to carry out the Box–Behnken design [57]:

$$N = 2K(K - 1) + cp \quad (3)$$

Where K is the number of process variables, and cp is the number of times the center point is repeated. The total number of trials in this study was 27, based on 3 levels and a 4 factor experimental design, with three replicates in the center of the design to estimate a sum of squares of pure error. Using Minitab 17 software, experimental data from a Box–Behnken design may be evaluated and fitted to a second-order polynomial model, Eq. 4 [58]:

$$Y = a_0 + \sum a_i x_i + \sum a_{ii} x_i^2 + \sum a_{ij} x_i x_j \quad (4)$$

Where Y is the Response Efficiency (RE %), i and j are the index numbers for independent variables,  $a_0$  is the intercept term, and  $x_1, x_2, x_k$  are the coded process variables (independent variables). The first-order (linear) main effect is denoted by  $a_i$ , the second-order main effect

by  $a_{ii}$ , and the interaction effect by  $a_{ij}$ . After analyzing variance, the regression coefficient ( $R^2$ ) was calculated to check the model's validity.

**Table 3.** Experimental Range and Levels of the Independent Variables

Variables	Levels in Box–Behnken design			
	Coded levels	Low(-1)	Middle(0)	High (+1)
X1-Applied voltage(v)		15	22.5	30
X2-flow rate (mL/min)		50	125	200
X3- pH		4	7	10
X4-GACMI dosage (g/L)		5	7.5	10

**Table 4.** Design Matrix in Coded and Experimental Units of the Parameters

Run	Blocks	Process variables (Coded value)				Process variables (Real value)			
		x1	x2	x3	x4	Voltage(v) X1	flow rate (mL/min) X2	pH X3	GACMI dosage (g/L) X4
1	1	0	1	0	-1	22.5	175.0	7	5.0
2	1	0	1	-1	0	22.5	175.0	4	7.5
3	1	1	1	0	0	30.0	175.0	7	7.5
4	1	1	0	0	-1	30.0	112.5	7	5.0
5	1	-1	-1	0	0	15.0	50.0	7	7.5
6	1	0	0	0	0	22.5	112.5	7	7.5
7	1	1	0	-1	0	30.0	112.5	4	7.5
8	1	0	1	0	1	22.5	175.0	7	10.0
9	1	0	0	-1	1	22.5	112.5	4	10.0
10	1	0	0	-1	-1	22.5	112.5	4	5.0
11	1	0	-1	-1	0	22.5	50.0	4	7.5
12	1	-1	0	-1	0	15.0	112.5	4	7.5
13	1	0	0	1	-1	22.5	112.5	10	5.0
14	1	0	0	0	0	22.5	112.5	7	7.5
15	1	1	0	1	0	30.0	112.5	10	7.5
16	1	-1	1	0	0	15.0	175.0	7	7.5
17	1	-1	0	0	1	15.0	112.5	7	10.0
18	1	0	-1	1	0	22.5	50.0	10	7.5
19	1	-1	0	0	-1	15.0	112.5	7	5.0
20	1	-1	0	1	0	15.0	112.5	10	7.5
21	1	1	0	0	1	30.0	112.5	7	10.0
22	1	0	-1	0	-1	22.5	50.0	7	5.0
23	1	0	0	0	0	22.5	112.5	7	7.5
24	1	1	-1	0	0	30.0	50.0	7	7.5
25	1	0	1	1	0	22.5	175.0	10	7.5
26	1	0	0	1	1	22.5	112.5	10	10.0
27	1	0	-1	0	1	22.5	50.0	7	10.0

### 3- Results and Discussion

#### 3.1. Textural Properties of Metal-Impregnated Activated Carbon

Based on nitrogen adsorption and desorption isotherms, Table 5 displays the physical characteristics of unprocessed GAC and GACMI (2:1) (specific surface area and total pore volume). It is evident that after the ferric-aluminum impregnation, GACMI (2:1)'s specific surface area and total pore volume both somewhat

decreased to 797.5  $m^2/g$  and 0.1376  $m^3/g$ , respectively. Metal oxides are distributed preferentially in the pore mouth, as shown by the decrease in these physical characteristic values. This leads to blocking certain micropores, creating meso- or macroporous structures, and binding binders to the active sites created by aluminum or ferric oxide [59].

The microstructural study provides relatively clear evidence for this as well. Fig. 2 displays a collection of SEM images of raw GAC (A1-4) and GACMI (2:1) (B1-4). It was found that when the raw GAC was impregnated

with metal, some porous structural collapse occurred, resulting in clogs, as is evident in Fig. 2 A1 to A3 and Fig. 2 B1 to B3, even though the porous structure of the raw GAC can be seen more clearly in Fig. 2 A1 to A4. Additionally, it is evident from Fig. 2 A4 that the surface of raw GAC before impregnation and picture B4 highlight the formation of metal oxide aggregates in spherical shapes on the surface of raw GAC following wet impregnation. Furthermore, for GACMI (2:1), it was determined that the average crystallite size of metal oxides fell between 18.75 and 26.89 nm. Image F4 shows that the range of metal oxide sizes was minimal and that the ferric and aluminum oxides were homogeneously aggregated on the surface of the raw GAC.

In addition to the SEM examination, an element analysis of the surface was carried out simultaneously with the EDX at the same surface regions. Table 6 shows the weight and atomic percentages of the raw GAC and MIGAC elements as determined from the EDX spectra. It is evident that for GACMI (2:1), the levels of Al and Fe were adjusted to 0.87% and 0.43%, respectively. The atomic percentage upon impregnation indicates that Al and Fe were fully impregnated into raw GAC. After impregnation, the Cl was sourced from  $\text{AlCl}_3$  and  $\text{FeCl}_3$ . Given the higher oxygen content in GACMI compared to raw GAC, it is acceptable to conclude that the Aluminum and Ferric elements were mostly bound to GACMI in the form of aluminum oxide and iron oxide. The metal oxide form in both raw GAC and GACMI must be verified, chemical analysis was done using XRF. The evidence of metal oxides forming on one another's surfaces is seen in Table 7. Table 7 shows Al and Fe are present, mainly in aluminum oxide and ferric oxide.

**Table 5.** Raw GAC and GACMI Microstructures

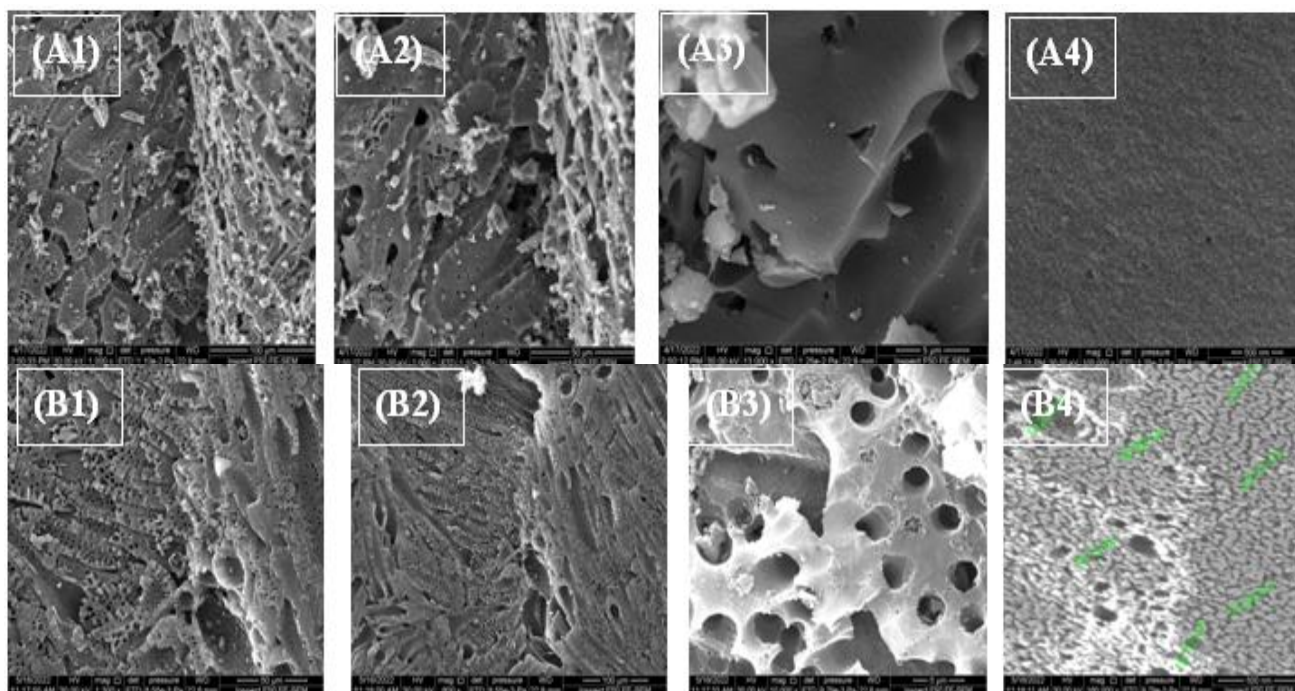
Parameters	GAC	GACMI (2:1)
BET specific surface area ( $\text{m}^2/\text{g}$ )	1086	797.5
Total pore volume ( $\text{cm}^3/\text{g}$ )	0.21702	0.01376

**Table 6.** TDX Elemental Contents of Raw GAC and GACMI

Element	GAC		GACMI(2:1)	
	Weight %	Atomic %	Weight %	Atomic %
C	88.82	92.7	73.95	83.6
O	7.28	5.7	13.33	11.3
Fe	-	-	1.65	0.43
Al	0.207	0.1	1.67	0.87
Si	1.78	0.8	0.21	0.1
Cl	-	-	9.02	3.6
K	1.51	0.5	-	-
Mg	0.38	0.2	0.18	0.1
Total	100	100	100	100

**Table 7.** XRF Analysis determined the Metal Oxide Form in both Raw GAC and GACMI

Components	GAC (mass%)	GACMI (2:1) (mass%)
MgO	0.4573	0.817
$\text{Al}_2\text{O}_3$	0.2899	3.3345
$\text{SiO}_2$	1.039	0.1765
$\text{P}_2\text{O}_5$	0.3564	0.1732
$\text{SO}_3$	0.09675	0.03716
Cl	0.05731	4.2253
$\text{K}_2\text{O}$	2.096	0.0666
CaO	2.919	1.239
$\text{TiO}_2$	0.00307	0.00466
$\text{V}_2\text{O}_5$	< 0.0011	< 0.00069
$\text{Cr}_2\text{O}_3$	< 0.00022	0.00099
MnO	0.00183	0.00326
$\text{Fe}_2\text{O}_3$	0.03133	1.7841
CoO	< 0.00039	< 0.00039
NiO	0.00081	0.00086
CuO	0.00318	0.00678
ZnO	0.00062	0.00162

**Fig. 2.** Scanning Electron Microscopy Images of (A1-4) GAC, and GACMI (2:1) (B1-4) at Different Expansion Ratios

### 3.2. Statistical Analysis

According to the feasibility test, which was done by Theydan and Mohammed [48], the best results were obtained for the activated carbon that was impregnated with metal salt (Al: Fe), which has a mass ratio (2:1) at a time of 40 min. However, there were no significant differences between the other systems. The results for the tested activated carbon may be explained by the possibility that polarized activated carbon increases the total active electrode surface when exposed to an electric field [60, 61].

The response surface methodology was employed by using Box-Behnken statistical experiment design to

investigate the effects of the four independent variables on the response function of the TEC-GACMI (2:1) system. The independent variables were applied voltage (X1), flow rate (X2), pH (X3), and GACMI (2:1) dosage (X4) at a constant time of 40 min.

The designed experiments were used to estimate the empirical correlations of the particular responses, the specifics of which are presented in Table 8 and Table 9. For the regression and graphic analysis of the results, Statistica-10 and Minitab-17 were used. A graphical description of statistical optimization by RSM was used to evaluate the interactive influence between the chosen factors and their impact on the outcomes.

**Table 8.** Experimental Results of Box-Behnken Design for Chemical Oxygen Demand Removal

Run	Blocks	Process variables (Coded value)				Process variables (Real value)				RE%			
		x <sub>1</sub>	x <sub>2</sub>	x <sub>3</sub>	x <sub>4</sub>	voltage(v)	flow rate (mL/min)	pH	GACMI dosage(g/L)	Actual	Predict	Turbidity Removal % (TR%)	Energy consumption (kWh/kg COD)
1	1	0	1	0	-1	22.5	175.0	7	5.0	81.600	81.836	96.823	1.324
2	1	0	1	-1	0	22.5	175.0	4	7.5	90.000	89.970	99.149	1.1939
3	1	1	1	0	0	30.0	175.0	7	7.5	93.000	92.807	98.643	2.434
4	1	1	0	0	-1	30.0	112.5	7	5.0	85.000	85.812	98.806	2.090
5	1	-1	-1	0	0	15.0	50.0	7	7.5	78.000	78.627	95.607	0.459
6	1	0	0	0	0	22.5	112.5	7	7.5	93.530	92.843	97.744	0.988
7	1	1	0	-1	0	30.0	112.5	4	7.5	93.600	93.981	98.713	2.143
8	1	0	1	0	1	22.5	175.0	7	10.0	90.000	91.809	98.854	1.408
9	1	0	0	-1	1	22.5	112.5	4	10.0	94.000	93.329	99.158	1.257
10	1	0	0	-1	-1	22.5	112.5	4	5.0	83.000	81.790	97.533	1.069
11	1	0	-1	-1	0	22.5	50.0	4	7.5	87.030	86.639	98.832	0.987
12	1	-1	0	-1	0	15.0	112.5	4	7.5	83.860	85.778	96.674	0.512
13	1	0	0	1	-1	22.5	112.5	10	5.0	76.920	78.025	96.444	1.313
14	1	0	0	0	0	22.5	112.5	7	7.5	93.000	92.843	97.744	0.993
15	1	1	0	1	0	30.0	112.5	10	7.5	90.000	88.331	97.682	2.069
16	1	-1	1	0	0	15.0	175.0	7	7.5	87.008	85.478	95.638	0.642
17	1	-1	0	0	1	15.0	112.5	7	10.0	88.500	87.002	97.801	0.469
18	1	0	-1	1	0	22.5	50.0	10	7.5	79.000	78.344	97.863	1.115
19	1	-1	0	0	-1	15.0	112.5	7	5.0	75.000	75.614	95.198	0.573
20	1	-1	0	1	0	15.0	112.5	10	7.5	80.000	79.868	98.321	0.537
21	1	1	0	0	1	30.0	112.5	7	10.0	94.770	93.470	99.207	2.539
22	1	0	-1	0	-1	22.5	50.0	7	5.0	78.000	76.440	96.528	1.102
23	1	0	0	0	0	22.5	112.5	7	7.5	92.000	92.843	97.744	1.004
24	1	1	-1	0	0	30.0	50.0	7	7.5	86.000	87.965	97.114	1.666
25	1	0	1	1	0	22.5	175.0	10	7.5	87.000	86.705	98.991	1.235
26	1	0	0	1	1	22.5	112.5	10	10.0	83.890	85.534	97.770	1.024
27	1	0	-1	0	1	22.5	50.0	7	10.0	85.500	85.513	98.013	1.256

It was shown that COD elimination efficiency ranges from 75 to 94.77 %. The turbidity removal efficiency ranges from (96.7 to 99.35 %) NTU. As demonstrated by the comparison of runs (4 and 21), where COD removal increased from 85 to 94.77% as the GACMI dose increased from 5 to 10 g/L at the applied voltage of 30 v and constant time of 40 min, it is evident that the GACMI dosage had a considerable impact on the effectiveness of COD removal. The comparison between runs (17 and 19) demonstrates that the effect of GACMI dose is more evident at a lower applied voltage (15 v), where COD elimination increased from 75 to 88.5% as GACMI dosage increased from 5 to 10 g/Comparison between runs (17 and 21) showed that the effect of the applied voltage is lower than the effect of GACMI dosage, where COD removal increased from 88.5 to 94.77 % as the applied voltage increased from 15 to 30 v. This

comparison demonstrates that rather than electrode reactions, the process is governed by the synergistic impact of the adsorption and electrocoagulation processes. On the other hand, the electrocoagulation reaction's performance would be improved by applying more voltage.

An experimental relationship between COD removal efficiency and process parameters was revealed and formulated using the results of COD removal efficiency analysis, which was carried out using Minitab-17 software. The quadratic model of COD removal efficiency (RE percent) in terms of un-coded (actual) units of process parameters was used:

$$RE\% = -41.4 + 3.048 X_1 + 0.2492 X_2 + 4.40 X_3 + 15.43 X_4 - 0.0449 X_1^2 - 0.001049 X_2^2 - 0.3699 X_3^2 - 0.775 X_4^2 - 0.00107 X_1 * X_2 + 0.0029 X_1 * X_3 - 0.0497 X_1 * X_4 + 0.00671 X_2 * X_3 + 0.00144 X_2 * X_4 - 0.134 X_3 * X_4 \quad (5)$$

Where X1, X2, X3, and X4 represent the applied voltage, flow rate, pH, and GACMI dosage, respectively, and RE% denotes the response or COD removal efficiency. In contrast, the variables X1X2, X1X3, X2X3, X2X4, and X3X4 show the interaction effect of all the model's parameters. The measures of the primary effects of the variables applied voltage, flow rate, pH, and GACMI dosage are  $(X1)^2$ ,  $(X2)^2$ ,  $(X3)^2$ , and  $(X4)^2$ , respectively.

Individual factors (linear and quadratic) or double interactions impact the COD removal efficiency, as shown in Eq. 5. Positive coefficient values indicated that COD removal effectiveness increased as the relevant variables of these coefficients grew within the investigated range, whilst negative coefficient values indicated the reverse impact. All factors have a favorable influence on COD removal efficiency, as observed. Predicted values of COD removal efficiency using Eq. 5 are also included in Table 9. Table 9 displays the response surface model's ANOVA results. Contribution percent (Cr. %), degree of freedom (DF), sum of squares (Seq. SS), the adjusted sum of squares (Adj. SS), adjusted mean of squares (Adj. MS), probability (P-value), and F-value are all evaluated in this table. The regression model was found to be highly significant with a P value of (0.000001) and a F value of (23.47). Regression can be

considered statistically significant given that the model's multiple correlation coefficient is 96.48%, and the model fails to validate only 3.39 percent of the total variants. This model's predicted multiple correlation coefficient was (pred.  $R^2$  =80.17%), which was quite close to the adjusted multiple correlation coefficient (adj.  $R^2$  =92.36%).

ANOVA results indicated that the GACMI dosage has the most significant effect on the process, with a contribution of 30.24%, followed by applied voltage with a contribution of 23.15 %, flow rate with a contribution of 11.40 %, and pH with a contribution of 11.14%. Evidently, the contribution of GACMI dosage has the greatest impact on COD elimination in the current investigation. Also, it was emphasized that pH has a statistically non-significant effect on the considered responses. This might be explained by the acidity of the surface functional groups of GACMI, which thus diminishes the impact of the initial pH of the solution treated. The contribution of the linear term to the model is the largest at 75.92 %, followed by the contribution of the square term at 18.88 % and the contribution of the 2-way interaction at 1.68%. The results indicated that interaction effects are considerable, with a total model contribution of (20.56%).

**Table 9.** Analysis of Variance for Chemical Oxygen Demand Removal

Source	DF	Seq SS	Contribution	Adj SS	Adj MS	F-Value	P-Value
<b>Model</b>	14	868.155	96.48%	868.155	62.011	23.47	0.000001
<b>Linear</b>	4	683.194	75.92%	683.194	170.798	64.63	0.000000
(X1)	1	208.344	23.15%	208.344	208.344	78.84	0.000001
(X2)	1	102.543	11.40%	102.543	102.543	38.80	0.000044
(X3)	1	100.225	11.14%	100.225	100.225	37.93	0.000049
(X4)	1	272.082	30.24%	272.082	272.082	102.96	0.000000
<b>Square</b>	4	169.869	18.88%	169.869	42.467	16.07	0.000092
X1*X1	1	0.032	0.00%	33.984	33.984	12.86	0.003740
X2*X2	1	27.053	3.01%	89.622	89.622	33.91	0.000082
X3*X3	1	17.635	1.96%	59.109	59.109	22.37	0.000489
X4*X4	1	125.149	13.91%	125.149	125.149	47.36	0.000017
<b>2-Way Interaction</b>	6	15.092	1.68%	15.092	2.515	0.95	0.495157
X1*X2	1	1.009	0.11%	1.009	1.009	0.38	0.548229
X1*X3	1	0.017	0.00%	0.017	0.017	0.01	0.937579
X1*X4	1	3.478	0.39%	3.478	3.478	1.32	0.273627
X2*X3	1	6.325	0.70%	6.325	6.325	2.39	0.147788
X2*X4	1	0.203	0.02%	0.203	0.203	0.08	0.786627
X3*X4	1	4.060	0.45%	4.060	4.060	1.54	0.238836
<b>Error</b>	12	31.710	3.52%	31.710	2.643		
<b>Lack-of-Fit</b>	10	30.503	3.39%	30.503	3.050	5.05	0.176405
<b>Pure Error</b>	2	1.207	0.13%	1.207	0.604		
<b>Total</b>	26	899.866	100.00%				
<b>Model summary</b>		S	R-sq	R-sq(adj)	PRESS	Rsq(pred)	
		1.62559	96.48%	92.36%	178.415	80.17%	

### 3.3. The Influence of Process Factors on COD Removal Efficiency

Graphical representations of the statistical optimization using RSM were used to evaluate the interactive effect of the chosen factors and their influence on the response.

Fig. 3 a, b illustrates the influence of GACMI dosage on COD removal efficiency at varying applied voltage (15-30 v) and constant pH (7), flow rate (112.5 mL/min), and time 30 min. Fig. 3 a depicts the response surface plot, whereas Fig. 3 b demonstrates the related contour plot. At

15 v, it is evident from the surface plot that the COD removal efficiency drops clearly when the GACMI dosage decreases from 10 to 5 g/L. By adjusting the applied voltage from 15 to 22.5 v at pH (7), flow rate (112.5 mL/min), and GACMI dosage 10 g/L, it was shown that the COD removal improved from 88.5% to 91.3%. The rise in voltage increases metal cations and bubble density in the solution, hence facilitating the removal of contaminants [14, 62]. COD removal increased marginally from 91.3 % to 94.77 % when the voltage was raised from 22.5 to 30 v at pH (7), flow rate

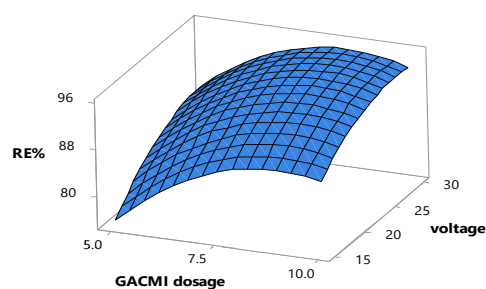
(112.5 mL/min), and GACMI (10 g/L). This was mostly due to the system's electrolysis efficiency being influenced by the quantity of particle electrodes introduced. Electrolysis efficiency decreases as the amount of activated carbon with metal impregnated added to the system decreases because fewer reaction sites are available and the lower Aluminum and ferric ions are dissolved. Because of the increased reaction sites provided by the activated carbon, the average mass transfer distance between the contaminants was reduced as activated carbon loading increased [63]. Additionally, pollution was removed at a higher rate, and this was due to the adsorption capacity of particle electrodes, which can extract pollutants on their surfaces, a rise in the production of amorphous  $\text{Al}(\text{OH})_3$  and  $\text{Fe}(\text{OH})_3$ . Hence, adequate performance was predicted. When subjected to an electric field, particle electrodes have improved water quality through adsorption and electrocoagulation [64].

In a three-dimensional electrochemical system, the current density is exactly proportional to the applied voltage, and this current density also affects the degradation process. Therefore, the applied voltage affects the COD removal. This discovery may most likely be explained by raising the applied voltage, which causes electrode particles to become more polarized, accelerating the oxidation and surface reduction potential processes [48, 65].

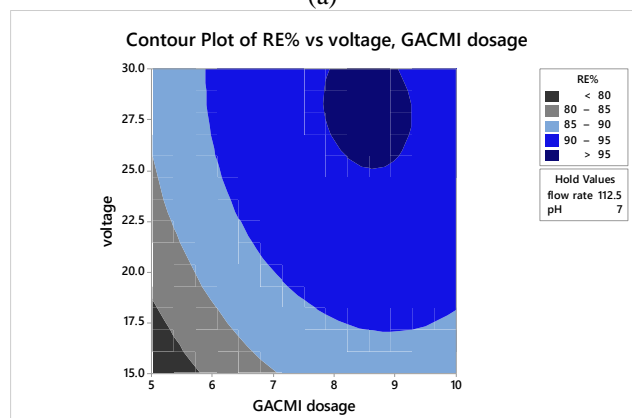
The primary reason for improving removal efficiency when using particle electrodes impregnated with metal ions ( $\text{Al}^+$  and  $\text{Fe}^+$ ) is the chains of microelectrodes in the electric field. These microelectrodes speed up the production of additional hydroxyl radicals, improving the effectiveness of both direct and indirect oxidation processes [66]. As the electrode dissolving rate increases, more  $\text{M}^+$  ions are released, and more electro-coagulants are formed, attracting and capturing colloidal and suspended particles in the wastewater. Eventually, as the electrolysis process progresses, the sludge at the top of the reactor will contain almost all of the pollutants that were removed from the wastewater throughout the electrolysis process. This was agreed with Uğurlu et al. [67], when they used a three-phase, three-dimensional (3D) electrode reactor to analyze the removal of color and COD from olive wastewater. They discovered that the maximum removal percentage was attained at 30 volts when the voltage was raised from 10 to 30 volts. It reached the rate of 85% color and COD removal after 90 minutes. These results were consistent with the present study's findings. The resulting contour plot reveals that the COD removal efficiency value of >95 % lies in a limited region when the applied voltage varied between 25.2 and 30v and the GACMI dosage varied between 7.8 and 9.3 g/L.

Fig. 4 a, b illustrates the influence of flow rates on COD removal efficiency at varying applied voltage (15-30 v), constant pH (7), GACMI dosage (7.5 g/L), and time 30 min. Fig. 4 a depicts the response surface plot, whereas Fig. 4 b demonstrates the related contour plot. At 15 v, it is evident from the surface plot that the COD removal efficiency is exponentially increased with increasing flow rate at a low applied voltage value. The same behavior

was observed as the applied voltage increased to 30 v. By adjusting the flow rate from 50 to 112.5 mL/min at an applied voltage (15 v), pH (7), and GACMI 7.5 g/L, it was shown that the COD removal improved from 78% to 86.5%. COD removal slightly increased from 92% to 93% when the flow rate was raised from 112.5 to 175 mL/min at an applied voltage (30 v), pH (7), and GACMI dosage (7.5 g/L). Pollutant removal is affected in numerous ways by the circulation rate. High circulation rates increase mass transfer and the number of contaminants that interact with the electrode's surface. In contrast, low circulation rates result in higher removal efficiencies with longer retention times [68]. The influence of flow rate on three dimensional is significant. The flow rate will affect the mass transfer process of the reaction. With the flow rate increase, diffusion and convection increase correspondingly, which is conducive to the increase of reaction rate [69]. The resulting contour plot reveals that the COD removal efficiency value of > 92.5 % lies in a limited region when the applied voltage varied between 21.3 and 30v and the flow rate ranged between 78.5 and 175 mL/min.



(a)

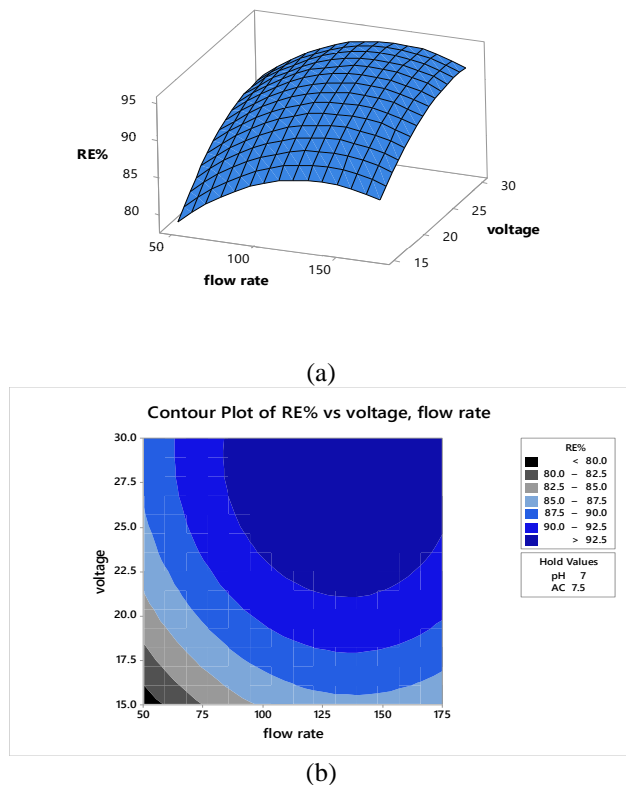


(b)

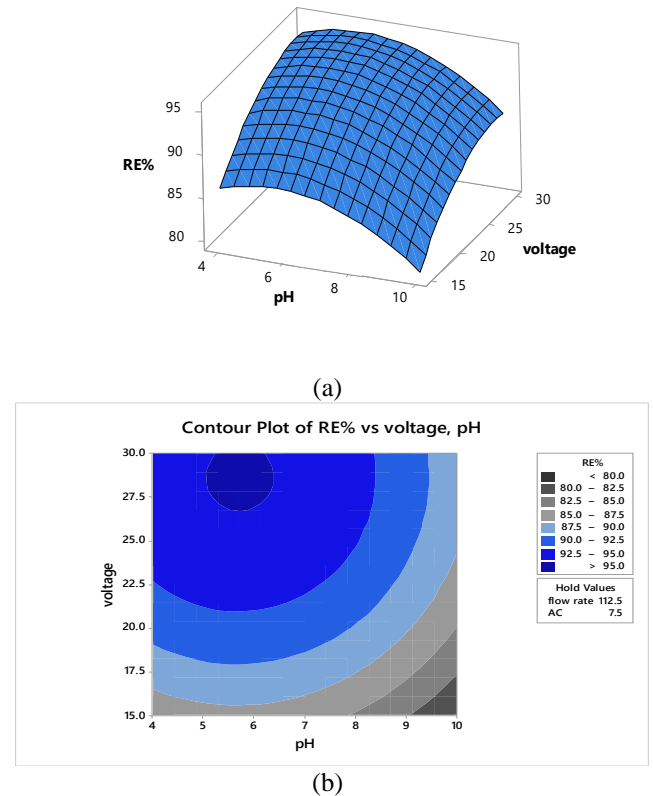
**Fig. 3.** Response Surface Plot (a) and Contour Plot (b) for the Impact of GACMI Dosage and Applied Voltage on the COD Removal Efficiency (RE%) (Hold Values: pH 7, Flow Rate 112.5 mL/min)

Fig. 5 a, b illustrate the effect of pH on COD removal efficiency for various applied voltages (15-30 v) at a constant flow rate (112.5 mL/min), GACMI dosage (7.5 g/L), and time 30 min. At a voltage of 15 v, the response

surface plot (5 -a) demonstrates that COD removal efficiency increases exponentially with increasing pH to 7. COD removal effectiveness decreased with rising pH. Adjusting the pH from 4 to 7 at applied voltage 22.5 v, flow rate (112.5 mL/min), and GACMI dosage (7.5 g/L) showed that the COD removal improved from 90 % to 93.53%. While COD removal decreased marginally from 93.53 % to 86.8 % when the pH was raised from 7 to 10 at applied voltage 22.5 v, flow rate (112.5 mL/min), and GACMI dosage (7.5 g/L). The initial pH is one of the most influential factors affecting the dominant metal hydroxide structure and the production of metal ions and hydroxyl ions. An increase in the creation of amorphous  $\text{Al}(\text{OH})_3$  and  $\text{Fe}(\text{OH})_3$  occurred as a result of the formation of a positively charged and stable colloidal precipitate in the pH range of 5-7, achievable performance was predicted, but at pH levels above optimum, the development of soluble  $\text{Al}(\text{OH})_4^-$  and  $\text{Fe}(\text{OH})_4^-$  should cause a drop in removal efficiency [ 48, 70]. The matching contour plot (5-b) verifies that the value of the COD removal efficiency >95 % lies in a limited area where the applied voltage varied between 26.8 and 30 v. The pH varied between 5 and 6.4. Fig. 6 displays the interaction plot between process partners. There were little significant interactions between the variables.



**Fig. 4.** Response Surface Plot (a) and Contour Plot (b) for the Impact of Flow Rate and Applied Voltage on the COD Removal Efficiency (RE%) (Hold Values: pH 7, GACMI Dosage 7.5 g/L)



**Fig. 5.** Response Surface Plot (a) and Contour Plot (b) for the Impact of pH Rate and Applied Voltage on the COD Removal Efficiency (RE%) (Hold Values: Flow Rate 112.5 mL/min, GACMI Dosage 7.5 g/L)

### 3.4. The Optimization and Confirmation Test

The independent parameters evaluated in this study were identified within the desired ranges (applied voltage: 15-30 v, flow rate: 50-175 mL/min, pH: 4-10, GACMI: 5-10 g/L, time=40 min). 75% was taken as the lowest limit of COD removal efficiency, while 94.77 percent was taken as the higher limit value. The optimisation technique was performed using these boundaries and parameters, and its results are shown in Table 10 with the desirability function of (1). To confirm optimization findings, two further runs were conducted; the results are shown in Table 11. After 40 minutes of electrolysis, a COD removal efficiency of 94.77 % as a mean value was attained at a pH of 7. This value is within the optimal range determined by optimization analysis with a desired function of (1) Table 10. Using the Box–Behnken design, with a desirability function, seems to be effective and efficient for maximizing COD removal in a three-dimensional electrocoagulation process with an aluminum electrode as a sacrificial anode and a stainless steel cathode operated at recirculating batch mode. Based on the findings of the present research. In the present work, COD removal efficiencies of 96.25 %, and turbidity removal efficiencies of 99 % were achieved based on the raw effluent properties.

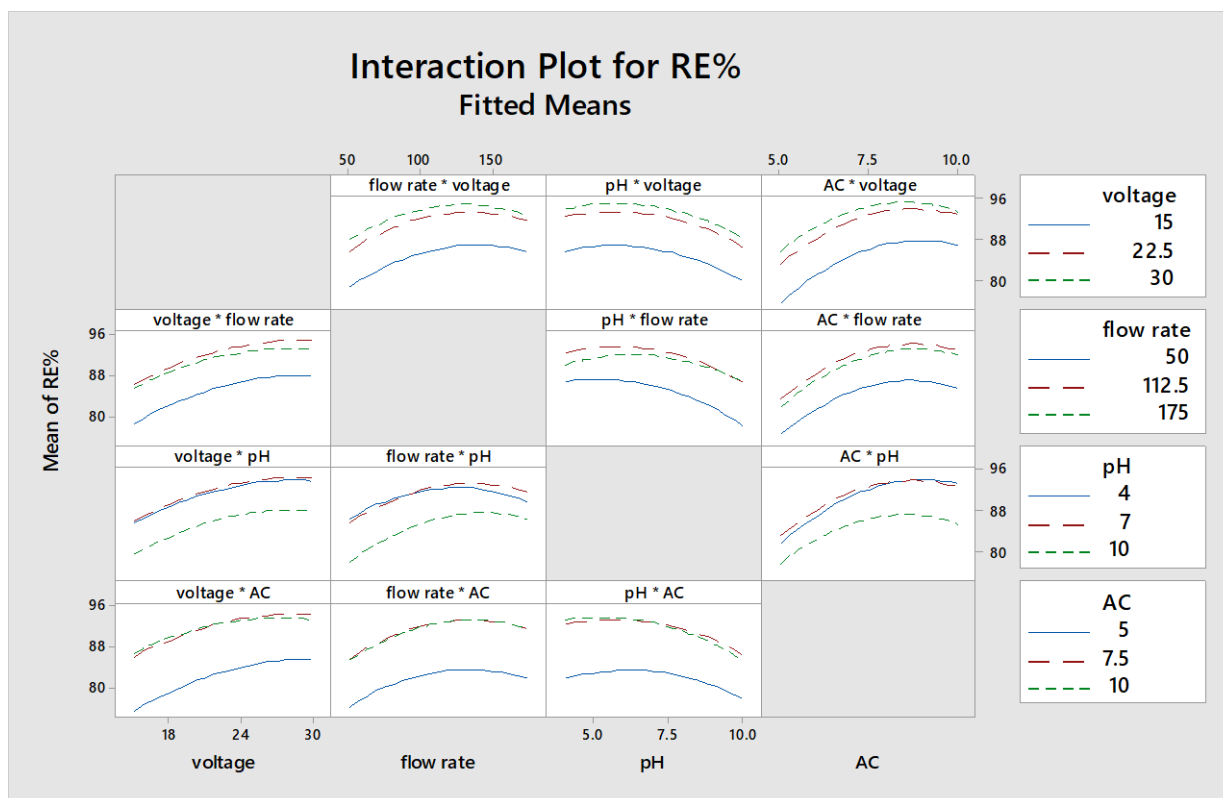


Fig. 6. Interaction Plot for COD Removal Efficiency (RE %)

Table 10. Optimization of Process Parameters for Optimal COD Removal Performance (RE %)

Response	Goal	Lower	Target	Upper	Weight	Importance
RE%	Maximum	75	Maximum	94.77	1	1
<b>Solution:</b>						
<b>Parameters</b>						
Voltage (Volt)	Flow rate (mL/min)	pH	GACMI dosage (g/L)	RE% fit	Composite desirability	SE Fit
27.7273	128.283	5.63636	8.68687	96.475	1	0.842
95% CI (94.640, 98.311)						
95% PI (92.486, 100.464)						

Table 11. Confirmation of the Optimal COD Removal Performance

Run	Applied voltage (v)	Flow rate (mL/min)	pH	GACMI Dosage (g/L)	Current density (mA/cm <sup>2</sup> )	COD (ppm)		RE%		Turbidity (NTU)		E (Kwh/kg COD)
						Initial	Final	Actual	Av.	Initial	Final	
1	27.7	128	5.6	8.7	11.32	1300	29.51	97.73	96.25	270	1.83	1.35
2	27.7	128	5.6	8.7	11.04	1300	68.12	94.76		270	2.71	1.32

#### 4- Conclusions

The present research examined the performance of a three electrocoagulation system operated at a batch recirculation mode under many operating factors such as applied voltage, the flow rate of recirculation, granule-activated carbon with metal-impregnated dosage and pH in the treatment of wastewater generated from Al-Dura petroleum refinery using Box-Behnken design as an optimization method. After the experimental data were fitted, a second-order polynomial equation was used to optimize the operational parameters. A COD removal efficiency of 96.25 % was achieved. An energy usage of 1.35 (kWh/kgCOD) was needed using the optimal operating parameters of voltage 27.7 v, flow rate 128 mL/min, pH 5.6, and granule-activated carbon with metal-

impregnated dosage 8.7 g/L. This comparison confirms that the process is controlled by a synergistic effect between the adsorption and electrocoagulation reactions rather than electrode reactions. However, increasing applied voltage would enhance the performance of the electrocoagulation reaction.

#### Acknowledgments

The authors would like to express their gratitude to the employees of the Chemical Engineering Department, College of Engineering, University of Baghdad, for their cooperation in carrying out this research.

## References

- [1] B. H. Diyaudden , W.M.A.W. Daud , and A.R. Abdul Aziz, “ Treatment Technologies for Petroleum Refinery Effluents: a Review”, *Process Safety and Environmental Protection*, vol. 89, no. 2, pp. 95–105, 2011 <https://doi.org/10.1016/j.psep.2010.11.003>
- [2] D. A. Aljuboury, P. Palaniandy, H.B. Abdul Aziz, and S. Feroz , “Treatment of petroleum wastewater by conventional and new technologies - A review”, *Global NEST Journal*, vol. 19 , no. 3 , pp. 439-452, 2017, <https://doi.org/10.30955/gnj.002239>
- [3] M. Al- Zarooni , and W. Elshorbagy, “Characterization and assessment of Al Ruwais refinery wastewater”, *Journal of Hazardous Materials*, vol. A136, pp. 398–405, 2006, <https://doi.org/10.1016/j.jhazmat.2005.09.060>
- [4] N. Shonza, D. Andreatta, E. Muniz, R. de Freitas, and P. Porto, “Crude oil wastewater treatment by electrocoagulation in a continuous process with polarity switch “, *Environmental Technology*, pp. 1-9, 2020, <https://doi.org/10.1080/09593330.2020.1847205>
- [5] A. H. Khalil, M. A. Naji, and S. M. Naser, “Removal of COD from petroleum refinery wastewater using electrocoagulation method”, *IOP Conference Series: Earth and Environmental Science*, vol. 877, 012046, 2021, <https://doi.org/10.1088/1755-1315/877/1/012046>
- [6] S. L. Zubaidi, H. Al-Bugharbee, Y. R. Muhsen, K. Hashim, R. M. Alkhaddar, D. Al-Jumeily, and A. J. Aljaaf, “The Prediction of Municipal Water Demand in Iraq: A Case Study of Baghdad Governorate”, *12th International Conference on Developments in eSystems Engineering (DeSE)*, Russia, 2019, <https://doi.org/10.1109/DeSE.2019.00058>
- [7] Z. Salah, K. Hashim, S. Ethaib, N. S. S. Al-Bdairi, H. Al-Bugharbee, and S. K. Gharghan, “A novel methodology to predict monthly municipal water demand based on weather variables scenario”, *Journal of King Saud University-Engineering Sciences*, vol. 32, pp. 1-18, 2020, <https://doi.org/10.1016/j.jksues.2020.09.011>
- [8] F. K. Attiogbe, M. Glover-Amengor, and K. T. Nyadziehe, “Correlating biochemical and chemical oxygen demand of effluents, a case study of selected industries in Kumasi Ghana”, *West African Journal Applied Ecology*, vol. 11, pp. 110-118, 2007, <https://doi.org/10.4314/wajae.v11i1.45722>
- [9] N. R. Kadhim, and M. Abdulredha , “Petroleum effluent treatment using electrocoagulation: A case study of phenols removal”, *IOP Conference Series: Materials Science and Engineering*, vol. 1184, 012009, 2021, <https://doi.org/10.1088/1757-899X/1184/1/012009>
- [10] H. Abbas, S. S. M. Al-Obaidy, Sh. Y. Al-Samarray, Kh. Edwan, A. Y. Al-Hayawi, and D. Yeboah , “Removal of phenols and COD from petroleum refinery wastewater using electrocoagulation method”, *IOP Conference Series: Materials Science and Engineering*, 2021, <https://doi.org/10.1088/1757-899X/1058/1/012005>
- [11] G. Moussavi, R. Khosravi, and M. Farzadkia, “Removal of petroleum hydrocarbons from contaminated groundwater using an electrocoagulation process: Batch and continuous experiments “, *Desalination*, vol. 278, pp. 288–294, 2011, <https://doi.org/10.1016/j.desal.2011.05.039>
- [12] I. K. Shakir, and B. I. Husein, B. I., “LEAD Removal from Industrial Wastewater by Electrocoagulation process”, *Iraqi Journal of Chemical and Petroleum Engineering* , vol. 10, no. 2, pp. 35-42, 2009, <https://doi.org/10.31699/IJCPE.2009.2.4>
- [13] U. Daiminger, W. Nitsch, P. Plucinski , and S. Hoffmann, “Novel techniques for oil/water separation “, *Journal of Membrane Science*, vol. 99, pp. 197–203, 1995, [https://doi.org/10.1016/0376-7388\(94\)00218-N](https://doi.org/10.1016/0376-7388(94)00218-N)
- [14] S. A. Martinez-Delgadillo, M. A. Morales-Mora, and I. D. Barcelo-Quintal, “Electrocoagulation treatment to remove pollutants from petroleum refinery wastewater “, *Sustainable Environment Research*, 20 (4), 227-231 2010.
- [15] M. A. Tony, P. J. Purcell, Y. Q. Zhao, A. M. Tayeb, and M. F. El-Sherbiny, “Photo-catalytic degradation of an oil-water emulsion using the photo-fenton treatment process: Effects and statistical optimization”, *Journal of Environmental Science and Health, Part A* , vol. A44 , no. 2, pp. 179-187, 2009, <https://doi.org/10.1080/10934520802539830>
- [16] C. E. Santo, V. J. P. Vilar, C. M. S. Botelho, K. E. Bhatnagar, and R. A. R. Boaventura, “Optimization of coagulation–flocculation and flotation parameters for the treatment of a petroleum refinery effluent from a Portuguese plant “, *Chemical Engineering Journal*, vol. 183, pp. 117– 123 , 2012, <https://doi.org/10.1016/j.cej.2011.12.041>
- [17] H. M. Ibrahim , and R. H. Salman, “Study the Optimization of Petroleum Refinery Wastewater Treatment by Successive Electrocoagulation and Electrooxidation Systems“, *Iraqi Journal of Chemical and Petroleum Engineering*, vol. 23, no. 1, pp. 31 – 41, 2022, <https://doi.org/10.31699/IJCPE.2022.1.5>
- [18] S. K. Theydan, and W. T. Mohammed, “An Electrocoagulation Process Operated at Batch Recirculation Mode for Treatment of Refinery Wastewaters: Optimization via Response Surface Methodology”, *Egyptian Journal of Chemistry*, vol.65, no. 13, 2022, <https://doi.org/10.21608/ejchem.2022.146203.6361>

- [19] S. S. Jawada, and A. H. Abbara, "Treatment of petroleum refinery wastewater by electrochemical oxidation using graphite anodes", *al- qadisiyah journal for engineering sciences*, vol. 12 ,pp. 144–150, 2019, <https://doi.org/10.30772/qjes.v12i3.609>
- [20] J. G. Jou, and G. G. Huang, "A pilot study for oil refinery wastewater treatment using a fixed film Bioreactor", *Advances in Environmental Research*, vol. 7, pp. 463–469, 2003, [https://doi.org/10.1016/S1093-0191\(02\)00016-3](https://doi.org/10.1016/S1093-0191(02)00016-3)
- [21] M. S. Kuyukina, A. V. Krivoruchko, and I. B. Ivshina, "Advanced Bioreactor Treatments of Hydrocarbon-Containing Wastewater", *Applied Sciences.*, vol. 10, no. 831, pp. 1-19, 2020, <http://dx.doi.org/10.3390/app10030831>
- [22] Sh. Jafarnejad, "Activated sludge combined with powdered activated carbon (PACT process) for the petroleum industry wastewater treatment", *Chemistry International*, vol. 3, no. 4, pp. 368-377, 2017, <https://doi.org/10.5281/zenodo.1473355>
- [23] G. Hu, J. Li, and H. Hou, "A combination of solvent extraction and freeze thaw for oil recovery from petroleum refinery wastewater treatment pond sludge", *Journal of Hazardous Materials*, vol. 283, pp. 832–840, 2015, <https://doi.org/10.1016/j.jhazmat.2014.10.028>
- [24] P. Stepnowski, E. M. Siedlecka, P. Behrend, and B. Jastorff, "Enhanced photo-degradation of contaminants in petroleum Refinery wastewater", *Water Research*, vol. 36, pp. 2167–2172, 2002, [https://doi.org/10.1016/S0043-1354\(01\)00450-X](https://doi.org/10.1016/S0043-1354(01)00450-X)
- [25] M. Y. A. Mollah, P. Morkovsky, J. A. G. Gomes, M. Kesmez, J. Parga, and D. L. Cocke, "Fundamentals, present and future perspectives of electrocoagulation", *Journal of Hazardous Materials*, vol. 114, pp. 199–210, 2004, <https://doi.org/10.1016/j.jhazmat.2004.08.009>
- [26] R. H. Salman, "Removal of Manganese Ions (Mn<sup>2+</sup>) from a Simulated Wastewater by Electrocoagulation/ Electroflotation Technologies with Stainless Steel Mesh Electrodes: Process Optimization Based on Taguchi Approach", *Iraqi Journal of Chemical and Petroleum Engineering*, vol. 20, no. 1, pp. 39 – 48, 2019, <https://doi.org/10.31699/IJCPE.2019.1.6>
- [27] M. Kobya, C. Ciftci, M. Bayramoglu, and M. Sensoy, "Study on the treatment of waste metal cutting fluids using electrocoagulation", *Separation and Purification Technology*, vol. 60, pp. 285–291, 2008, <https://doi.org/10.1016/j.seppur.2007.09.003>
- [28] A. S. Al-Nuaimi, and K. S. Pak, "Chromium (VI) Removal from Wastewater by Electrocoagulation Process Using Taguchi Method: Batch Experiments", *Iraqi Journal of Chemical and Petroleum Engineering*, vol. 17, no. 4, pp. 95- 103, 2016, <https://doi.org/10.31699/IJCPE.2016.4.9>
- [29] F. Özyonar, "Treatment of Oily Wastewater by Electrocoagulation Process and Optimization of the Experimental Conditions Using Taguchi Method", *Cumhuriyet Sciences Journal*, vol. 39, no. 4, pp. 1127-1135, 2018, <http://dx.doi.org/10.17776/csj.395844>
- [30] S. H. Ammar, N. N. Ismail, A. D. Ali, and W. M. Abbas, "Electrocoagulation technique for refinery wastewater treatment in an internal loop split-plate airlift reactor", *Journal of Environmental Chemical Engineering*, vol. 7, no. 6, 2019, <https://doi.org/10.1016/j.jece.2019.103489>
- [31] V. Khandegar, and A. K. Saroha, "Electrocoagulation for the treatment of textile industry effluent – a review", *Journal of Environmental Management*, vol. 128, pp. 949–963, 2013, <https://doi.org/10.1016/j.jenvman.2013.06.043>
- [32] R. Katal, and H. Pahlavanzadeh, "Influence of different combinations of aluminum and iron electrode on electrocoagulation efficiency: application to the treatment of paper mill wastewater", *Desalination*, vol. 265, pp. 199–205, 2011, <https://doi.org/10.1016/j.desal.2010.07.052>
- [33] C. Zhang, Y. Jiang, Y. Li, Z. Hu, L. Zhou, and M. Zhou, "Three-dimensional electrochemical process for wastewater treatment: A general review", *Chemical Engineering Journal*, 2013, <https://doi.org/10.1016/j.cej.2013.05.033>
- [34] K. U. Altuntas, "Fluidized Electrooxidation Process Using Three-Dimensional Electrode for Decolorization of Reactive Blue 221", *Academic Platform Journal of Engineering and Science*, vol. 9 no. 1, pp. 53-58, 2021, <http://dx.doi.org/10.21541/apjes.782973>
- [35] R. Misra, N. N. Neti, D. D. Dionysiou, M. Tandekar, and G. S. Kanade, "Novel integrated carbon particle based three dimensional anodes for the electrochemical degradation of reactive dyes", *RSC Advances*, vol. 5 no. 14, pp. 10799–10808, 2015, <https://doi.org/10.1039/C4RA13550D>
- [36] Y. Sun, P. Li, H. Zheng, Ch. Zhao, X. Xiao, Y. Xu, W. Sun, Wu. H. Huifang, and M. Ren, "Electrochemical treatment of chloramphenicol using Ti-Sn/c-Al<sub>2</sub>O<sub>3</sub> particle electrodes with a three-dimensional reactor", *Chemical Engineering Journal*, vol. 308, pp.1233-1242, 2017, <https://doi.org/10.1016/j.cej.2016.10.072>
- [37] M. Paidar, K. Bouzek, M. Laurich, and J. Thonstad, "Application of a Three-Dimensional Electrode to the Electrochemical Removal of Copper and Zinc Ions from Diluted Solutions", *Water Environment Research*, vol. 72, no. 5, pp. 618-625, 2000, <http://dx.doi.org/10.2175/106143000X138201>

- [38] S. Yonghui, L. Siming, Y. Ning, and H. Wenjin, "Treatment Cyanide Wastewater Dynamic Cycle Test by Three-dimensional Electrode System and the Reaction Process Analysis", *Environmental Technology*, vol. 42, no. 11, 2021, <https://doi.org/10.1080/09593330.2019.1677783>
- [39] S. T. Kadhum, G. Y. Alkindi, and T. M. Albayati, "Remediation of phenolic wastewater implementing nano zerovalent iron as a granular third electrode in an electrochemical reactor", *International Journal of Environmental Science and Technology*, vol. 19, pp. 1383–1392, 2022, <https://doi.org/10.1007/s13762-021-03205-5>
- [40] S. Sowmiya, R. Gandhimathi, S. Th. Ramesh, and P. V. Nidheesh, "Granular Activated Carbon as a Particle Electrode in Three-Dimensional Electrochemical Treatment of Reactive Black B from Aqueous Solution", *Environmental Progress & Sustainable Energy*, vol. 35, no. 6, pp. 1616–1622, 2016, <https://doi.org/10.1002/ep.12396>
- [41] R. Shokoohi, M. Foroughi, Z. Latifi, H. Goljani, A. Ansari, M. R. Samarghandi, and D. Nematollahi, "Comparing the performance of the peroxymonosulfate/Mn<sub>3</sub>O<sub>4</sub> and three-dimensional electrochemical processes for methylene blue removal from aqueous solutions: Kinetic studies", *Colloid and Interface Science Communications*, vol. 42, pp. 100394, 2021, <https://doi.org/10.1016/j.colcom.2021.100394>
- [42] Sh. Tang, M. Zhao, D. Yuan, X. Li, Z. Wang, X. Zhang, T. Jiao, and J. Ke, "Fe<sub>3</sub>O<sub>4</sub> nanoparticles three-dimensional electro-peroxydisulfate for improving tetracycline degradation", *Chemosphere*, vol. 268, pp. 1–12, 2021, <https://doi.org/10.1016/j.chemosphere.2020.129315>
- [43] P. Pourali, M. Fazlzadeh, M. Aaligadri, A. Dargahi, Y. Poureshgh, and B. Kakavandi, "Enhanced three-dimensional electrochemical process using magnetic recoverable of Fe<sub>3</sub>O<sub>4</sub>@GAC towards furfural degradation and mineralization", *Arabian Journal of Chemistry*, vol. 15, pp. 103980, 2022, <https://doi.org/10.1016/j.arabjc.2022.103980>
- [44] B. Y. Tak, B. S. Tak, Y. J. Kim, Y. J. Park, Y. H. Yoon, and G. H. Min, "Optimization of Color and COD Removal from Livestock Wastewater by Electrocoagulation Process: Application of Box – Behnken Design (BBD)", *Journal of Industrial and Engineering Chemistry*, vol. 28, pp. 307–315, 2015, <https://doi.org/10.1016/j.jiec.2015.03.008>
- [45] V. Preethia, S. Th. Ramesha, R. Gandhimathia, and P. V. Nidheesh, "Optimization of batch electrocoagulation process using Box-Behnken experimental design for the treatment of crude vegetable oil refinery wastewater", *Journal of Dispersion Science and Technology*, 2019, <https://doi.org/10.1080/01932691.2019.1595640>
- [46] R. B. A. Souza, L. A. M. Ruotolo, R. B. A. Souza, and L. A. M. Ruotolo, "Electrochemical treatment of oil refinery effluent using boron-doped diamond anodes", *Journal of Environmental Chemical Engineering*, vol. 1, no. 3, pp. 544–551, 2013, <https://doi.org/10.1016/j.jece.2013.06.020>
- [47] S. K. Theydan, and W. T. Mohammed, "Refinery Wastewater Treatment by a Novel Three-Dimensional Electrocoagulation System Design", *Engineering, Technology & Applied Science Research*, vol. 12, no. 6, pp. 9590–9600, 2022, <https://doi.org/10.48084/etasr.5316>
- [48] K. W. Jung, M. J. Hwang, D. S. Park, and K. H. Ahn, "Performance evaluation and optimization of a fluidized three dimensional electrode reactor combining pre-exposed granular activated carbon as a moving particle electrode for greywater treatment", *Separation and Purification Technology*, vol. 156, no. 2, pp. 414–423, 2015, <https://doi.org/10.1016/j.seppur.2015.10.030>
- [49] E. Gengec, M. Kobya, E. Demirbas, A. Akyol, and K. Oktor, "Electrochemical treatment of Baker's yeast wastewater containing melanoidin: Optimization through response surface methodology", *Water Science and Technology*, vol. 65, no. 12, pp. 2183–2190, 2012, <https://doi.org/10.2166/wst.2012.130>
- [50] J. B. Parsa, H. R. Vahidian, A. R. Soleymani, and M. Abbasi, "Removal of Acid Brown 14 in aqueous media by electrocoagulation: optimization parameters and minimizing of energy consumption", *Desalination*, vol. 278, pp. 295–302, 2011, <https://doi.org/10.1016/j.desal.2011.05.040>
- [51] S. H. Ammar, F. D. Ali, R. F. Shafi, and A. I. Elaibi, "Zn(II) Removal from Wastewater by Electrocoagulation/Flotation Method using New Configuration of a Split-Plate Airlift Electrochemical Reactor", *Journal of Engineering*, vol. 24, no. 1, pp. 97–110, 2018, <http://dx.doi.org/10.31026/j.eng.2018.01.07>
- [52] D. S. Ibrahim, P. S. Devi, and N. Balasubramanian, "Electrochemical Oxidation Treatment of Petroleum Refinery Effluent", *International Journal of Scientific & Engineering Research*, pp. 4–8, 2013.
- [53] D. C. Montgomery, "Design and analysis of experiments, Response Surface Methods and Designs", chapter 11, 8<sup>th</sup> edition. John Wiley & Sons, Inc., New York, 2013.
- [54] J. Antony, "Design of experiments for engineers and scientists, Fundamentals of Design of Experiments", chapter 2, 1st Edition, Butterworth Heinemann, Oxford, 2014, <https://doi.org/10.1016/B978-0-08-099417-8.00002-X>
- [55] J. He, L. Zhu, C. Liu, and Q. Bai, "Optimization of the oil agglomeration for high-ash content coal slime based on design and analysis of response surface methodology (RSM)", *Fuel*, vol. 254, pp. 115560, 2019, <https://doi.org/10.1016/j.fuel.2019.05.143>

- [56] H. Zhang, Y. Li, X. Wu, Y. Zhang, and D. Zhang, "Application of response surface methodology to the treatment landfill leachate in a three-dimensional electrochemical reactor", *Waste Management*, vol. 30, pp. 2096–2102, 2010, <https://doi.org/10.1016/j.wasman.2010.04.029>
- [57] K. Tarangini, A. Kumar, G. R. Satpathy, and V. K. Sangal, "Statistical optimization of process parameters for Cr (VI) biosorption onto mixed cultures of *Pseudomonas aeruginosa* and *Bacillus subtilis*", *Clean-Soil Air Water*, vol. 37, pp. 319–327, 2009, <https://doi.org/10.1002/clen.200900033>
- [58] V. Preethia, S. Th. Ramesha, R. Gandhimathia, and P. V. Nidheesh, "Optimization of batch electrocoagulation process using Box-Behnken experimental design for the treatment of crude vegetable oil refinery wastewater", *Journal Of Dispersion Science And Technology*, 2019, <https://doi.org/10.1080/01932691.2019.1595640>
- [59] U. Balasubramani, R. Venkatesh, S. Subramaniam, G. Gopalakrishnan, and V. Sundararajan, "Alumina/Activated Carbon Nano-composites: Synthesis and Application in Sulphide Ion Removal from Water", *Journal of Hazardous Materials*, vol. 340, pp. 241–252, 2017, <http://dx.doi.org/doi:10.1016/j.jhazmat.2017.07.006>
- [60] H. Ghanbarlou, N. L. Pedersen, M. E. Simonsen, and J. Mu, "Nitrogen-Doped Graphene Iron-Based Particle Electrode Outperforms Activated Carbon in Three-Dimensional Electrochemical Water Treatment Systems", *Water*, vol. 12, 3121, 2020, <https://doi.org/10.3390/w12113121>
- [61] N. L. Pedersen, F. M. Nikbakht, P. K. Molnar, and J. Muff, "Synergy of combined adsorption and electrochemical degradation of aqueous organics by granular activated carbon particulate electrodes", *Separation and Purification Technology*, vol. 208, pp. 51–58, 2019, <https://doi.org/10.1016/J.SEPUR.2018.05.023>
- [62] E. Can-Güven, "Advanced treatment of dye manufacturing wastewater by electrocoagulation and electro-fenton processes: effect on COD fractions, energy consumption, and sludge analysis", *Journal of Environmental Management*, vol. 300, 113784, 2021, <https://doi.org/10.1016/j.jenvman.2021.113784>
- [63] W. Li, W. Wang, and P. Zhang, "Three-Phase Three-Dimensional Electrochemical Process for Efficient Treatment of Greywater", *Membranes*, vol. 12, 514, 2022, <https://doi.org/10.3390/membranes12050514>
- [64] X. Zhu, J. Ni, X. Xing, H. Li, and Y. Jiang, "Synergies between electrochemical oxidation and activated carbon adsorption in three-dimensional boron-doped diamond anode system", *Electrochimica Acta*, vol. 56, pp. 1270–1274, 2011, <http://dx.doi.org/10.1016/j.electacta.2010.10.073>
- [65] C. T. Wang, J. L. Hu, W. L. Chou, and Y. M. Kuo, "Removal of color from real dyeing wastewater by electro-Fenton technology using a three-dimensional graphite cathode", *Journal of Hazardous Materials*, vol. 152, pp. 601–606, 2008, <https://doi.org/10.1016/j.jhazmat.2007.07.023>
- [66] S. Singh, Sh. Mahesh, and M. Sahana, "Three-dimensional batch electrochemical coagulation (ECC) of health care facility wastewater—clean water reclamation", *Environmental Science and Pollution Research*, 2019, <https://doi.org/10.1007/s11356-019-04789-9>
- [67] M. Uğurlu, S. I. Yilmaz, and A. Vaizoğullar, "Removal of Color and COD from Olive Wastewater by Using Three-Phase Three-Dimensional (3D) Electrode Reactor", *Materials Today: Proceedings*, vol. 18, pp. 1986–1995, 2019, <https://doi.org/10.1016/j.matpr.2019.06.690>
- [68] R. F. Brocenschi, R. C. Rocha-Filho, N. Bocchi, and S. R. Biaggio, "Electrochemical degradation of estrone using a borondoped diamond anode in a filter-press reactor", *Electrochim Acta*, vol. 197, pp. 186–193, 2016, <https://doi.org/10.1016/j.electacta.2015.09.170>
- [69] J. Cheng, H. Haitao -Yang, Ch. Fan, R. Li, X. Xiaohua Yu, and Li. H. Hongtao "Review on the applications and development of fluidized bed electrodes", *Journal of Solid State Electrochemistry*, 2020, <https://doi.org/10.1007/s10008-020-04786-w>
- [70] S. Safari, A. M. Azadi, and H-R. Kariminia, "Electrocoagulation for COD and diesel removal from oily wastewater", *International Journal of Environmental Science and Technology*, vol. 13, pp. 231–242, 2016, <https://doi.org/10.1007/s13762-015-0863-5>

## تحسين عملية التخثير الكهربائي ثلاثي الابعاد التي تعمل بنظام اعادة تدوير الدفعات باستخدام منهجية الاستجابة السطحية لمعالجة مياه الصرف الصحي للمصافي النفطية

سمر كريم زيدان<sup>١\*</sup>، ودود طاهر<sup>١</sup>، شيخ مانيرول حقي<sup>٢</sup>

<sup>١</sup> قسم الهندسة الكيماوية، كلية الهندسة، جامعة بغداد، بغداد، العراق

<sup>٢</sup> قسم الهندسة الكيماوية، جامعة جيبيل، المملكة العربية السعودية

### الخلاصة

اداء عملية التخثير الكهربائي ثلاثية الابعاد التي يتم تشغيلها في وضع اعادة التدوير على دفعات لمعالجة مياه الصرف الصحي المطروحة من مصفاة تكرير البترول سوف يتم التحقق منها في هذه الدراسة باستخدام الالمنيوم كقطب الانود، والستانلس ستيل كقطب الكاثود والكربون المشبع بالمعدن ((GACMI(1:2) مع نسبة وزنية (1Al:2Fe) كقطب ثالث. تم دراسة تأثيرات عوامل التشغيل مثل الجهد المطبق (١٥-٣٠ فولت)، معدل تدفق (٥٠-١٧٥ مل/ دقيقة)، pH (٤-١٠)، وكمية GACMI (٥-١٠ غم/ لتر) على ازالة متطلب الاكسجين الكيماوي (COD). باستخدام تصميم Box-Behnken، تم انشاء نموذج رياضي يتعلق بالمعايير التشغيلية الاساسية لتقليل متطلب الاكسجين الكيماوي. حيث اظهرت النتائج ان تأثير كمية GACMI على كفاءة ازالة COD كان كبيرا حيث زادت ازالة ال COD مع زيادة كمية GACMI ومع ذلك، فان زيادة الجهد المطبق سيعزز اداء فعالية التخثر الكهربائي. تم تحقيق ازالة متطلب الاكسجين الكيماوي ٩٦,٢٥% تحت الظروف المثلى (الجهد المطبق = ٢٧,٧ فولت، معدل تدفق = ١٢٨ مل/ دقيقة، pH = ٥,٦، وكمية GACMI = ٨,٧ غم /لتر). تم استخدام فحص BET المساحة السطحية وحجم المسام الكلية وفحص الاشعة السينية (XRF) وفحص مطيافية الاشعة السينية المشتتة للطاقة (EDX) والفحص المجهر الالكتروني (SEM) لتوصيف اقطاب جسيمات GACMI.

الكلمات الدالة: التخثر الكهربائي ثلاثي الابعاد، منهجية الاستجابة السطحية، نظام اعادة تدوير الدفعات، مياه الصرف الصحي للمصافي النفطية.